LETTER

doi:10.1038/nature09466

A two-solar-mass neutron star measured using Shapiro delay

P. B. Demorest[1], T. Pennucci[2], S. M. Ransom[1], M. S. E. Roberts[3] & J. W. T. Hessels[4,5]

Neutron stars are composed of the densest form of matter known to exist in our Universe, the composition and properties of which are still theoretically uncertain. Measurements of the masses or radii of these objects can strongly constrain the neutron star matter equation of state and rule out theoretical models of their composition[1,2]. The observed range of neutron star masses, however, has hitherto been too narrow to rule out many predictions of 'exotic' non-nucleonic components[3–6]. The Shapiro delay is a general-relativistic increase in light travel time through the curved space-time near a massive body[7]. For highly inclined (nearly edge-on) binary millisecond radio pulsar systems, this effect allows us to infer the masses of both the neutron star and its binary companion to high precision[8,9]. Here we present radio timing observations of the binary millisecond pulsar J1614-2230[10,11] that show a strong Shapiro delay signature. We calculate the pulsar mass to be $(1.97 \pm 0.04)M_{\odot}$, which rules out almost all currently proposed[2–5] hyperon or boson condensate equations of state ($M_{\odot}$, solar mass). Quark matter can support a star this massive only if the quarks are strongly interacting and are therefore not 'free' quarks[12].

In March 2010, we performed a dense set of observations of J1614-2230 with the National Radio Astronomy Observatory Green Bank Telescope (GBT), timed to follow the system through one complete 8.7-d orbit with special attention paid to the orbital conjunction, where the Shapiro delay signal is strongest. These data were taken with the newly built Green Bank Ultimate Pulsar Processing Instrument (GUPPI). GUPPI coherently removes interstellar dispersive smearing from the pulsar signal and integrates the data modulo the current apparent pulse period, producing a set of average pulse profiles, or flux-versus-rotational-phase light curves. From these, we determined pulse times of arrival using standard procedures, with a typical uncertainty of $\sim$1 μs.

We used the measured arrival times to determine key physical parameters of the neutron star and its binary system by fitting them to a comprehensive timing model that accounts for every rotation of the neutron star over the time spanned by the fit. The model predicts at what times pulses should arrive at Earth, taking into account pulsar rotation and spin-down, astrometric terms (sky position and proper motion), binary orbital parameters, time-variable interstellar dispersion and general-relativistic effects such as the Shapiro delay (Table 1). We compared the observed arrival times with the model predictions, and obtained best-fit parameters by χ^2 minimization, using the TEMPO2 software package[13]. We also obtained consistent results using the original TEMPO package. The post-fit residuals, that is, the differences between the observed and the model-predicted pulse arrival times, effectively measure how well the timing model describes the data, and are shown in Fig. 1. We included both a previously recorded long-term data set and our new GUPPI data in a single fit. The long-term data determine model parameters (for example spin-down rate and astrometry) with characteristic timescales longer than a few weeks, whereas the new data best constrain parameters on timescales of the orbital period or less. Additional discussion of the long-term data set, parameter covariance and dispersion measure variation can be found in Supplementary Information.

As shown in Fig. 1, the Shapiro delay was detected in our data with extremely high significance, and must be included to model the arrival times of the radio pulses correctly. However, estimating parameter values and uncertainties can be difficult owing to the high covariance between many orbital timing model terms[14]. Furthermore, the χ^2 surfaces for the Shapiro-derived companion mass (M_2) and inclination angle (i) are often significantly curved or otherwise non-Gaussian[15]. To obtain robust error estimates, we used a Markov chain Monte Carlo (MCMC) approach to explore the post-fit χ^2 space and derive posterior probability distributions for all timing model parameters (Fig. 2). Our final results for the model

Table 1 | Physical parameters for PSR J1614-2230

Parameter	Value
Ecliptic longitude (λ)	245.78827556(5)°
Ecliptic latitude (β)	−1.256744(2)°
Proper motion in λ	9.79(7) mas yr^{-1}
Proper motion in β	−30(3) mas yr^{-1}
Parallax	0.5(6) mas
Pulsar spin period	3.1508076534271(6) ms
Period derivative	$9.6216(9) \times 10^{-21}$ s s^{-1}
Reference epoch (MJD)	53,600
Dispersion measure*	34.4865 pc cm^{-3}
Orbital period	8.6866194196(2) d
Projected semimajor axis	11.2911975(2) light s
First Laplace parameter ($e\sin\omega$)	$1.1(3) \times 10^{-7}$
Second Laplace parameter ($e\cos\omega$)	$-1.29(3) \times 10^{-6}$
Companion mass	$0.500(6)M_{\odot}$
Sine of inclination angle	0.999894(5)
Epoch of ascending node (MJD)	52,331.1701098(3)
Span of timing data (MJD)	52,469–55,330
Number of TOAs†	2,206 (454, 1,752)
Root mean squared TOA residual	1.1 μs
Right ascension (J2000)	16 h 14 min 36.5051(5) s
Declination (J2000)	−22° 30′ 31.081(7)″
Orbital eccentricity (e)	$1.30(4) \times 10^{-6}$
Inclination angle	89.17(2)°
Pulsar mass	$1.97(4)M_{\odot}$
Dispersion-derived distance‡	1.2 kpc
Parallax distance	>0.9 kpc
Surface magnetic field	1.8×10^{8} G
Characteristic age	5.2 Gyr
Spin-down luminosity	1.2×10^{34} erg s^{-1}
Average flux density* at 1.4 GHz	1.2 mJy
Spectral index, 1.1–1.9 GHz	−1.9(1)
Rotation measure	−28.0(3) rad m^{-2}

Timing model parameters (top), quantities derived from timing model parameter values (middle) and radio spectral and interstellar medium properties (bottom). Values in parentheses represent the 1σ uncertainty in the final digit, as determined by MCMC error analysis. The fit included both 'long-term' data spanning seven years and new GBT–GUPPI data spanning three months. The new data were observed using an 800-MHz-wide band centred at a radio frequency of 1.5 GHz. The raw profiles were polarization- and flux-calibrated and averaged into 100-MHz, 7.5-min intervals using the PSRCHIVE software package[25], from which pulse times of arrival (TOAs) were determined. MJD, modified Julian date.
* These quantities vary stochastically on $\gtrsim$1-d timescales. Values presented here are the averages for our GUPPI data set.
† Shown in parentheses are separate values for the long-term (first) and new (second) data sets.
‡ Calculated using the NE2001 pulsar distance model[26].

[1]National Radio Astronomy Observatory, 520 Edgemont Road, Charlottesville, Virginia 22093, USA. [2]Astronomy Department, University of Virginia, Charlottesville, Virginia 22094-4325, USA. [3]Eureka Scientific, Inc., Oakland, California 94602, USA. [4]Netherlands Institute for Radio Astronomy (ASTRON), Postbus 2, 7990 AA Dwingeloo, The Netherlands. [5]Astronomical Institute ''Anton Pannekoek'', University of Amsterdam, 1098 SJ Amsterdam, The Netherlands.

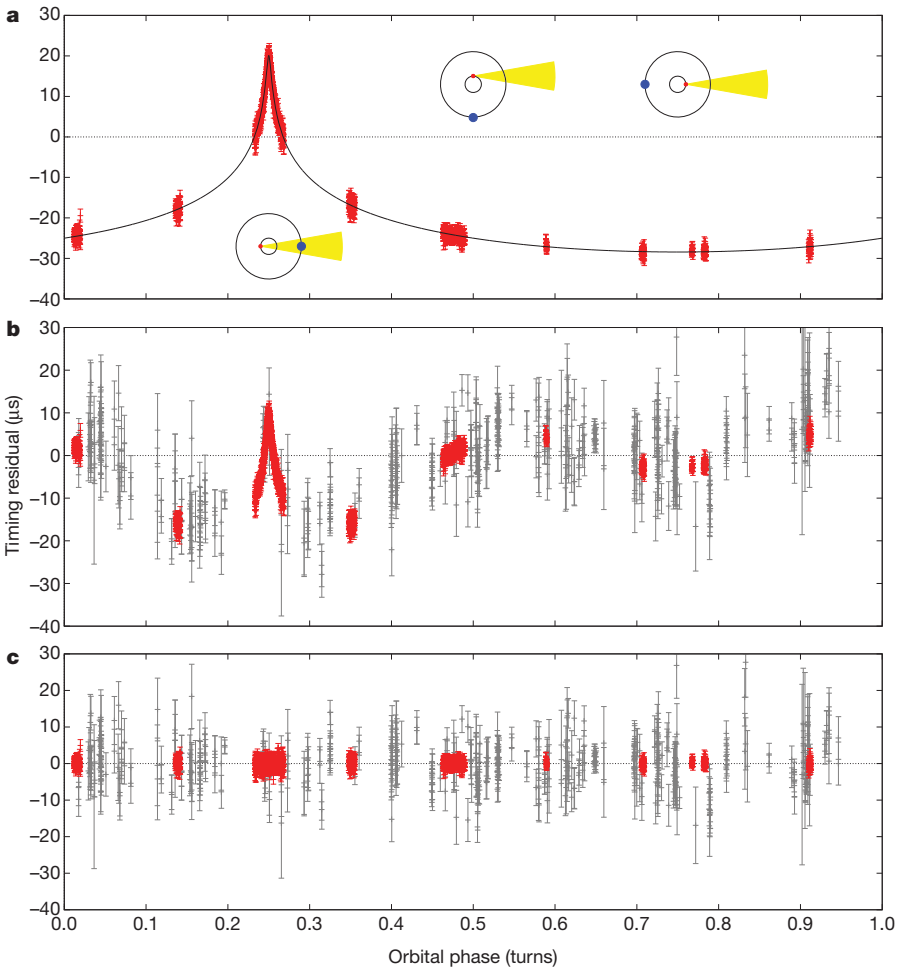

Figure 1 | Shapiro delay measurement for PSR J1614-2230. Timing residual—the excess delay not accounted for by the timing model—as a function of the pulsar's orbital phase. **a**, Full magnitude of the Shapiro delay when all other model parameters are fixed at their best-fit values. The solid line shows the functional form of the Shapiro delay, and the red points are the 1,752 timing measurements in our GBT–GUPPI data set. The diagrams inset in this panel show top-down schematics of the binary system at orbital phases of 0.25, 0.5 and 0.75 turns (from left to right). The neutron star is shown in red, the white dwarf companion in blue and the emitted radio beam, pointing towards Earth, in yellow. At orbital phase of 0.25 turns, the Earth–pulsar line of sight passes nearest to the companion (~240,000 km), producing the sharp peak in pulse delay. We found no evidence for any kind of pulse intensity variations, as from an eclipse, near conjunction. **b**, Best-fit residuals obtained using an orbital model that does not account for general-relativistic effects. In this case, some of the Shapiro delay signal is absorbed by covariant non-relativistic model parameters. That these residuals deviate significantly from a random, Gaussian distribution of zero mean shows that the Shapiro delay must be included to model the pulse arrival times properly, especially at conjunction. In addition to the red GBT–GUPPI points, the 454 grey points show the previous 'long-term' data set. The drastic improvement in data quality is apparent. **c**, Post-fit residuals for the fully relativistic timing model (including Shapiro delay), which have a root mean squared residual of 1.1 μs and a reduced χ^2 value of 1.4 with 2,165 degrees of freedom. Error bars, 1σ.

parameters, with MCMC error estimates, are given in Table 1. Owing to the high significance of this detection, our MCMC procedure and a standard χ^2 fit produce similar uncertainties.

From the detected Shapiro delay, we measure a companion mass of $(0.500 \pm 0.006)M_{\odot}$, which implies that the companion is a helium–carbon–oxygen white dwarf[16]. The Shapiro delay also shows the binary system to be remarkably edge-on, with an inclination of $89.17^{\circ} \pm 0.02^{\circ}$. This is the most inclined pulsar binary system known at present. The amplitude and sharpness of the Shapiro delay increase rapidly with increasing binary inclination and the overall scaling of the signal is linearly proportional to the mass of the companion star. Thus, the unique combination of the high orbital inclination and massive white dwarf companion in J1614-2230 cause a Shapiro delay amplitude orders of magnitude larger than for most other millisecond pulsars. In addition, the excellent timing precision achievable from the pulsar with the GBT and GUPPI provide a very high signal-to-noise ratio measurement of both Shapiro delay parameters within a single orbit.

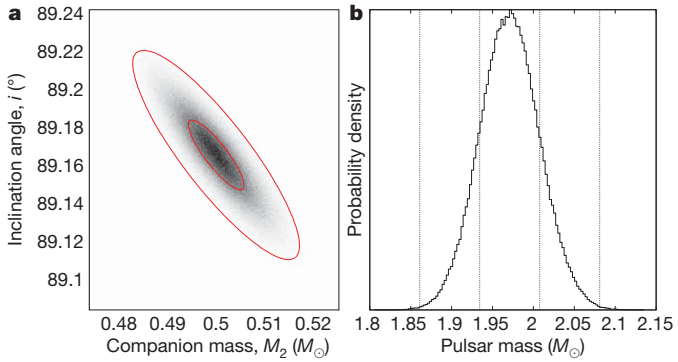

Figure 2 | Results of the MCMC error analysis. **a**, Grey-scale image shows the two-dimensional posterior probability density function (PDF) in the M_2–i plane, computed from a histogram of MCMC trial values. The ellipses show 1σ and 3σ contours based on a Gaussian approximation to the MCMC results. **b**, PDF for pulsar mass derived from the MCMC trials. The vertical lines show the 1σ and 3σ limits on the pulsar mass. In both cases, the results are very well described by normal distributions owing to the extremely high signal-to-noise ratio of our Shapiro delay detection. Unlike secular orbital effects (for example precession of periastron), the Shapiro delay does not accumulate over time, so the measurement uncertainty scales simply as $T^{-1/2}$, where T is the total observing time. Therefore, we are unlikely to see a significant improvement on these results with currently available telescopes and instrumentation.

The standard Keplerian orbital parameters, combined with the known companion mass and orbital inclination, fully describe the dynamics of a 'clean' binary system—one comprising two stable compact objects—under general relativity and therefore also determine the pulsar's mass. We measure a pulsar mass of $(1.97 \pm 0.04)M_{\odot}$, which is by far the highest precisely measured neutron star mass determined to date. In contrast with X-ray-based mass/radius measurements[17], the Shapiro delay provides no information about the neutron star's radius. However, unlike the X-ray methods, our result is nearly model independent, as it depends only on general relativity being an adequate description of gravity. In addition, unlike statistical pulsar mass determinations based on measurement of the advance of periastron[18–20], pure Shapiro delay mass measurements involve no assumptions about classical contributions to periastron advance or the distribution of orbital inclinations.

The mass measurement alone of a $1.97M_{\odot}$ neutron star significantly constrains the nuclear matter equation of state (EOS), as shown in Fig. 3. Any proposed EOS whose mass–radius track does not intersect the J1614-2230 mass line is ruled out by this measurement. The EOSs that produce the lowest maximum masses tend to be those which predict significant softening past a certain central density. This is a

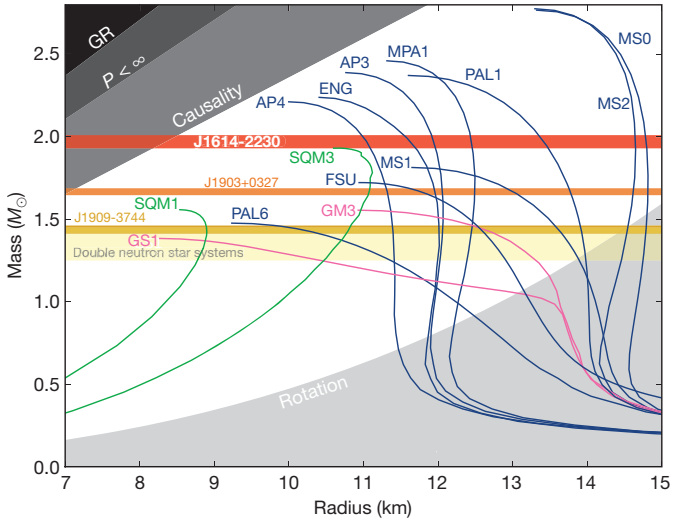

Figure 3 | Neutron star mass–radius diagram. The plot shows non-rotating mass versus physical radius for several typical EOSs[27]: blue, nucleons; pink, nucleons plus exotic matter; green, strange quark matter. The horizontal bands show the observational constraint from our J1614-2230 mass measurement of $(1.97 \pm 0.04)M_\odot$, similar measurements for two other millisecond pulsars[8,28] and the range of observed masses for double neutron star binaries[2]. Any EOS line that does not intersect the J1614-2230 band is ruled out by this measurement. In particular, most EOS curves involving exotic matter, such as kaon condensates or hyperons, tend to predict maximum masses well below $2.0M_\odot$ and are therefore ruled out. Including the effect of neutron star rotation increases the maximum possible mass for each EOS. For a 3.15-ms spin period, this is a $\lesssim$2% correction[29] and does not significantly alter our conclusions. The grey regions show parameter space that is ruled out by other theoretical or observational constraints[2]. GR, general relativity; P, spin period.

common feature of models that include the appearance of 'exotic' hadronic matter such as hyperons[4,5] or kaon condensates[3] at densities of a few times the nuclear saturation density (n_s), for example models GS1 and GM3 in Fig. 3. Almost all such EOSs are ruled out by our results. Our mass measurement does not rule out condensed quark matter as a component of the neutron star interior[6,21], but it strongly constrains quark matter model parameters[12]. For the range of allowed EOS lines presented in Fig. 3, typical values for the physical parameters of J1614-2230 are a central baryon density of between $2n_s$ and $5n_s$ and a radius of between 11 and 15 km, which is only 2–3 times the Schwarzschild radius for a $1.97M_\odot$ star. It has been proposed that the Tolman VII EOS-independent analytic solution of Einstein's equations marks an upper limit on the ultimate density of observable cold matter[22]. If this argument is correct, it follows that our mass measurement sets an upper limit on this maximum density of $(3.74 \pm 0.15) \times 10^{15}\,\mathrm{g\,cm^{-3}}$, or $\sim 10n_s$.

Evolutionary models resulting in companion masses $>0.4M_\odot$ generally predict that the neutron star accretes only a few hundredths of a solar mass of material, and result in a mildly recycled pulsar[23], that is one with a spin period >8 ms. A few models resulting in orbital parameters similar to those of J1614-2230[23,24] predict that the neutron star could accrete up to $0.2M_\odot$, which is still significantly less than the $\gtrsim 0.6M_\odot$ needed to bring a neutron star formed at $1.4M_\odot$ up to the observed mass of J1614-2230. A possible explanation is that some neutron stars are formed massive ($\sim 1.9M_\odot$). Alternatively, the transfer of mass from the companion may be more efficient than current models predict. This suggests that systems with shorter initial orbital periods and lower companion masses—those that produce the vast majority of the fully recycled millisecond pulsar population[23]—may experience even greater amounts of mass transfer. In either case, our mass measurement for J1614-2230 suggests that many other millisecond pulsars may also have masses much greater than $1.4M_\odot$.

Received 7 July; accepted 1 September 2010.

1. Lattimer, J. M. & Prakash, M. The physics of neutron stars. *Science* **304,** 536–542 (2004).
2. Lattimer, J. M. & Prakash, M. Neutron star observations: prognosis for equation of state constraints. *Phys. Rep.* **442,** 109–165 (2007).
3. Glendenning, N. K. & Schaffner-Bielich, J. Kaon condensation and dynamical nucleons in neutron stars. *Phys. Rev. Lett.* **81,** 4564–4567 (1998).
4. Lackey, B. D., Nayyar, M. & Owen, B. J. Observational constraints on hyperons in neutron stars. *Phys. Rev. D* **73,** 024021 (2006).
5. Schulze, H., Polls, A., Ramos, A. & Vidaña, I. Maximum mass of neutron stars. *Phys. Rev. C* **73,** 058801 (2006).
6. Kurkela, A., Romatschke, P. & Vuorinen, A. Cold quark matter. *Phys. Rev. D* **81,** 105021 (2010).
7. Shapiro, I. I. Fourth test of general relativity. *Phys. Rev. Lett.* **13,** 789–791 (1964).
8. Jacoby, B. A., Hotan, A., Bailes, M., Ord, S. & Kulkarni, S. R. The mass of a millisecond pulsar. *Astrophys. J.* **629,** L113–L116 (2005).
9. Verbiest, J. P. W. *et al.* Precision timing of PSR J0437–4715: an accurate pulsar distance, a high pulsar mass, and a limit on the variation of Newton's gravitational constant. *Astrophys. J.* **679,** 675–680 (2008).
10. Hessels, J. *et al.* in *Binary Radio Pulsars* (eds Rasio, F. A. & Stairs, I. H.) 395 (ASP Conf. Ser. 328, Astronomical Society of the Pacific, 2005).
11. Crawford, F. *et al.* A survey of 56 midlatitude EGRET error boxes for radio pulsars. *Astrophys. J.* **652,** 1499–1507 (2006).
12. Özel, F., Psaltis, D., Ransom, S., Demorest, P. & Alford, M. The massive pulsar PSR J1614−2230: linking quantum chromodynamics, gamma-ray bursts, and gravitational wave astronomy. *Astrophys. J.* (in the press).
13. Hobbs, G. B., Edwards, R. T. & Manchester, R. N. TEMPO2, a new pulsar-timing package - I. An overview. *Mon. Not. R. Astron. Soc.* **369,** 655–672 (2006).
14. Damour, T. & Deruelle, N. General relativistic celestial mechanics of binary systems. II. The post-Newtonian timing formula. *Ann. Inst. Henri Poincaré Phys. Théor.* **44,** 263–292 (1986).
15. Freire, P. C. C. & Wex, N. The orthometric parameterisation of the Shapiro delay and an improved test of general relativity with binary pulsars. *Mon. Not. R. Astron. Soc.* (in the press).
16. Iben, I. Jr & Tutukov, A. V. On the evolution of close binaries with components of initial mass between 3 solar masses and 12 solar masses. *Astrophys. J Suppl. Ser.* **58,** 661–710 (1985).
17. Özel, F. Soft equations of state for neutron-star matter ruled out by EXO 0748 - 676. *Nature* **441,** 1115–1117 (2006).
18. Ransom, S. M. *et al.* Twenty-one millisecond pulsars in Terzan 5 using the Green Bank Telescope. *Science* **307,** 892–896 (2005).
19. Freire, P. C. C. *et al.* Eight new millisecond pulsars in NGC 6440 and NGC 6441. *Astrophys. J.* **675,** 670–682 (2008).
20. Freire, P. C. C., Wolszczan, A., van den Berg, M. & Hessels, J. W. T. A massive neutron star in the globular cluster M5. *Astrophys. J.* **679,** 1433–1442 (2008).
21. Alford, M. *et al.* Astrophysics: quark matter in compact stars? *Nature* **445,** E7–E8 (2007).
22. Lattimer, J. M. & Prakash, M. Ultimate energy density of observable cold baryonic matter. *Phys. Rev. Lett.* **94,** 111101 (2005).
23. Podsiadlowski, P., Rappaport, S. & Pfahl, E. D. Evolutionary sequences for low- and intermediate-mass X-ray binaries. *Astrophys. J.* **565,** 1107–1133 (2002).
24. Podsiadlowski, P. & Rappaport, S. Cygnus X-2: the descendant of an intermediate-mass X-Ray binary. *Astrophys. J.* **529,** 946–951 (2000).
25. Hotan, A. W., van Straten, W. & Manchester, R. N. PSRCHIVE and PSRFITS: an open approach to radio pulsar data storage and analysis. *Publ. Astron. Soc. Aust.* **21,** 302–309 (2004).
26. Cordes, J. M. & Lazio, T. J. W. NE2001.I. A new model for the Galactic distribution of free electrons and its fluctuations. Preprint at ⟨http://arxiv.org/abs/astro-ph/0207156⟩ (2002).
27. Lattimer, J. M. & Prakash, M. Neutron star structure and the equation of state. *Astrophys. J.* **550,** 426–442 (2001).
28. Champion, D. J. *et al.* An eccentric binary millisecond pulsar in the Galactic plane. *Science* **320,** 1309–1312 (2008).
29. Berti, E., White, F., Maniopoulou, A. & Bruni, M. Rotating neutron stars: an invariant comparison of approximate and numerical space-time models. *Mon. Not. R. Astron. Soc.* **358,** 923–938 (2005).

Supplementary Information is linked to the online version of the paper at www.nature.com/nature.

Acknowledgements P.B.D. is a Jansky Fellow of the National Radio Astronomy Observatory. J.W.T.H. is a Veni Fellow of The Netherlands Organisation for Scientific Research. We thank J. Lattimer for providing the EOS data plotted in Fig. 3, and P. Freire, F. Özel and D. Psaltis for discussions. The National Radio Astronomy Observatory is a facility of the US National Science Foundation, operated under cooperative agreement by Associated Universities, Inc.

Author Contributions All authors contributed to collecting data, discussed the results and edited the manuscript. In addition, P.B.D. developed the MCMC code, reduced and analysed data, and wrote the manuscript. T.P. wrote the observing proposal and created Fig. 3. J.W.T.H. originally discovered the pulsar. M.S.E.R. initiated the survey that found the pulsar. S.M.R. initiated the high-precision timing proposal.

Author Information Reprints and permissions information is available at www.nature.com/reprints. The authors declare no competing financial interests. Readers are welcome to comment on the online version of this article at www.nature.com/nature. Correspondence and requests for materials should be addressed to P.B.D. (pdemores@nrao.edu).